LUND UNIVERSITY

Binding Affinities of Factor Xa Inhibitors Estimated by Thermodynamic Integration and MM/GBSA.

Genheden, Samuel; Nilsson, Ingemar; Ryde, Ulf

Published in:
Journal of Chemical Information and Modeling

DOI:
10.1021/ci100458f

2011

Link to publication

Citation for published version (APA):
Genheden, S., Nilsson, I., & Ryde, U. (2011). Binding Affinities of Factor Xa Inhibitors Estimated by Thermodynamic Integration and MM/GBSA. *Journal of Chemical Information and Modeling*, *51*(Online March 18, 2011), 947-958. https://doi.org/10.1021/ci100458f

Total number of authors:
3

General rights
Unless other specific re-use rights are stated the following general rights apply:
Copyright and moral rights for the publications made accessible in the public portal are retained by the authors and/or other copyright owners and it is a condition of accessing publications that users recognise and abide by the legal requirements associated with these rights.
• Users may download and print one copy of any publication from the public portal for the purpose of private study or research.
• You may not further distribute the material or use it for any profit-making activity or commercial gain
• You may freely distribute the URL identifying the publication in the public portal

Read more about Creative commons licenses: https://creativecommons.org/licenses/

Take down policy
If you believe that this document breaches copyright please contact us providing details, and we will remove access to the work immediately and investigate your claim.

LUND UNIVERSITY

PO Box 117
221 00 Lund
+46 46-222 00 00

Download date: 09. Sep. 2026

Binding affinities of factor Xa inhibitors estimated by thermodynamic integration and MM/GBSA

Samuel Genheden[1], Ingemar Nilsson[2], Ulf Ryde[1*]

[1]Department of Theoretical Chemistry, Lund University, Chemical Centre, P. O. Box 124, SE-221 00 Lund, Sweden

[2]Medicinal Chemistry, AstraZeneca R&D, SE-431 83 Mölndal, Sweden

*Correspondence to Ulf Ryde, E-mail: Ulf.Ryde@teokem.lu.se, Tel: +46 – 46 2224502, Fax: +46 – 46 2224543

2012-02-03

Abstract
We present free energy estimates of nine 3-amidinobenzyl-1*H*-indole-2-carboxamide inhibitors of factor Xa. Using alchemical thermodynamic integration (TI) calculations, we estimate the difference in binding free energies with high accuracy and precision, except for mutations involving one of the amidinobenzyl rings. Crystal studies show that the inhibitors may bind in two distinct conformations and using TI, we show that the two conformations give a similar binding affinity. Furthermore we show that we can reduce the computational demand, while still retaining a high accuracy and precision, by using fewer integration points and shorter protein–ligand simulations. Finally, we have compared the TI results to those obtained with the simpler MM/GBSA method (molecular-mechanics with generalised Born surface-area solvation). MM/GBSA gives better results for the mutations that involve a change of net charge, but if a precision similar to that of the TI method is required, the MM/GBSA method is actually slightly more expensive. Thus, we have shown that TI could be a valuable tool in drug design.

Introduction

Myocardial infarction, pulmonary embolism, and stroke are among the leading causes of death in the industrialised parts of the world. They are triggered by undesirable clot formation within blood vessels. The clot formation is initiated by an intricate series of enzymatic reactions that eventually generate fibrin.[1,2] Some of the current medicinal treatment of these cardiovascular diseases target this cascade, but are frustrated with serious side-effects, such as toxicity and interference between different drugs.[3] Traditionally, research has been focused on the inhibition of thrombin, but lately much effort has been directed towards the inhibition of the enzyme factor Xa.[1,4]

Factor Xa (fXa) is a serine protease that converts prothrombin to thrombin, which then catalyses the reactions that lead to the production of blood clots. Therefore, by inhibiting fXa, the blood coagulation cascade can be halted. This cascade works by amplification in such a way that a single fXa molecule can generate many molecules of thrombin, and the inhibition of fXa may therefore be more efficient than the inhibition of thrombin.[1,2,5] In particular, fXa seems to have a wider therapeutic window between unwanted haemorrhage and thrombosis.[6,7] Hence, research into more effective fXa inhibitors is highly motivated.

Computational methods can aid such research and help rationalising experimental findings. There exist many methods to calculate the binding affinity of a ligand, e.g., an inhibitor, to a receptor, e.g., a protein, ranging from statistical and empirical scoring functions to rigours simulation-based methods that are founded on the laws of statistical mechanics. Scoring functions are fast, but fail to give good results on a wide range of systems.[8] Therefore, we will concentrate on physics-based methods that are based on detailed simulations of the system of interest.

One of the most rigours of these methods is thermodynamic integration (TI).[9] With this method, it is possible to calculate accurate differences in binding free energies between two related ligand with a high accuracy and precision. In some instances, absolute free energies can also be calculated.[10] However, this method requires extensive sampling of unphysical, intermediate states, and therefore is computationally demanding, which explains why it has been little used in drug design.[11]

Instead, several simplified methods have been developed that are still based on simulations, but only sample the end-points of the reaction, e.g. PDLD/s-LRA[12] (semi-macroscopic protein-dipole and Langevin-dipole within a linear response approximation), LIE[13] (linear interaction energy), and MM/GBSA[14,15] (molecular-mechanics coupled with generalised Born surface-area solvation). The latter method is interesting because it is composed of physically well-defined terms and contains no adjustable parameters. It has been shown to be useful to estimate binding affinities,[16,17,18,19] although it sometimes fails.[20,21] A problem with this method has been the high statistical uncertainty of the estimates.[22] However, recently, we have shown how this can be reduced and how statistically converged results can be obtained.[23,24] This is mandatory if you want to compare MM/GBSA with other methods.

In this paper we study the binding of nine inhibitors to fXa using TI and MM/GBSA. Several sets of fXa inhibitors have been previously studied with rigorous free energy methods,[3,25,26] LIE,[3,27] empirical scoring functions,[28,29] and QSAR.[4] We have chosen to study a set of 3-amidinobenzyl-1*H*-indole-2-carboxamide inhibitors, for which both accurate binding data and crystal structures are available.[2] We show how the protocol for performing TI can be systematically tuned to decrease the computational demand, while still retaining a high accuracy and precision. When an optimal protocol has been found, the results are compared to those obtained with the MM/GBSA approach.

Methods

Preparation of the molecular systems

A set of nine 3-amidinobenzyl-1*H*-indole-2-carboxamide inhibitors was selected (denoted by bold numbers according to the numbering in ref. 2) and they are shown in Figure 1. Ligands **39, 57** and **63** have single positive charge, whereas the other six have a double positive charge. The simulations are based on the crystal structure of fXa in complex with **125**.[2] The other eight inhibitors were manually built in the active site by replacing atoms or groups of the ligand **125**. These binding modes were also independently confirmed by docking calculations using DOCK6.[30] The crystal structure of the fXa–**125** complex shows two distinct conformations of the ligand with equal occupancy, caused by a 180° rotation of one of the amidinobenzyl groups. Therefore, both conformations were considered in this study and they will be referred to as A and B (Figure 2).

The preparation of the receptor has been described previously:[23] All Asp and Glu residues were considered to have a negative charge and all the Arg and Lys residues were considered to have a positive charge. The histidine residues were protonated in the following way: Residues 57 and 83 were protonated on the $N^{\delta 1}$ atom, residues 91, 145, and 199 on the $N^{\varepsilon 2}$ atom, and residue 13 on both atoms. This gave a net charge for the free protein of +2. No counter ions were added in the simulations. The protein was described by the Amber99 force field[31] and the inhibitors by the generalised Amber force field[32] with charges derived from a restrained electrostatic potential-procedure (RESP)[33] using ESP points calculated at the Hartree–Fock 6-31G* level and sampled with the Merz–Kollman scheme.[34]

The protein–ligand complexes or the isolated ligands were immersed in a truncated octahedral box of TIP3P waters[35] that extended at least 10 Å from the solute.

Thermodynamic-integration calculations

Relative binding free energies were calculated using the thermodynamic cycle in Figure 3. From this cycle, we can calculate the difference in binding free energy between ligand 1 (L1) and ligand 2 (L2) as

$$\Delta\Delta G_{bind} = \Delta G_{bind}(\mathrm{L2}) - \Delta G_{bind}(\mathrm{L1}) = \Delta G_{bound}(\mathrm{L1}\rightarrow\mathrm{L2}) - \Delta G_{free}(\mathrm{L1}\rightarrow\mathrm{L2}) \qquad (1)$$

where ΔG_{bind} is the binding free energy and $\Delta G(\mathrm{L1}\rightarrow\mathrm{L2})$ is the free energy of mutating L1 into L2, either when they are bound to the receptor or when then they are free in solution. The mutations considered are shown in Figure 1.

The $\Delta G(\mathrm{L1}\rightarrow\mathrm{L2})$ energy differences are calculated using alchemical thermodynamic integration. Two variants of this approach were used. In the first, the process is divided into three transformations that we will call T1, T2, and T3. In T1, charges on atoms that change in the mutation are zeroed. In T2, the van der Waals parameters of the mutated atoms are changed, keeping the charges zeroed. Simultaneously, charges on the other atoms in the ligand are changed from those of L1 to those of L2 (in general, the RESP charges for the two ligands differ for all atoms, not only for the mutated atoms). Finally, in T3, L2 charges are introduced also on the mutated atoms. To avoid end-point problems in T2 (when atoms disappear), a soft-core version of the Lennard-Jones potential, as implemented in the Amber simulation package, was used.[36] This protocol using three transformations will be called the three-transformation approach (TTA) in the following.

A soft-core version of also the Coulomb potential was recently introduced in the Amber simulation package. This makes it possible to do both the charge and van der Waals mutations in the same step, and we will call this the single transformation-approach (STA).

To improve the convergence of the free-energy difference, the mutation of L1 to L2 was

divided into several small steps, involving intermediate states, and total free energy of all transformations was calculated using

$$\Delta G = \int_0^1 \langle \frac{\delta V}{\delta \lambda} \rangle_\lambda \, d\lambda \qquad (2)$$

where the brackets indicate an average over snapshots from an MD trajectory and V is defined as $V(\lambda) = (1-\lambda)V_0 + \lambda V_1$ where V_0 and V_1 is the potential energy of the L1 and L2 states, respectively. As a standard, nine λ values were used (0.1, 0.2, 0.3, 0.4, 0.5, 0.6, 0.7, 0.8, and 0.9), but we test different numbers of λ values. Data for λ = 0 and 1 were obtained by a linear interpolation using the two closest values. The integral in Eqn. 2 was estimated by the trapezoid method. In all calculations, we use a dual-topology scheme with two sets of coordinates for the atoms that differ between L1 and L2.

With such a scheme, we can actually also calculate the difference in binding free energies of the two conformations (A and B) for each ligand (in this case, we employ the same topology for the two states, but different coordinates for the atoms in the amidinobenzyl group as well as the joining CH_2 group).[37] We denote the free energy of changing the conformation of a ligand from the A to the B conformation ΔG_{conf}. All TI calculations were performed with the Amber software, versions 10[38] (TTA) or 11[39] (STA).

MM/GBSA calculations

The MM/GBSA method estimates the binding free energy of a ligand, L, by[14,15]

$$\Delta G_{bind}(\mathrm{L}) = \langle G(PL) \rangle - \langle G(P) \rangle - \langle G(L) \rangle \qquad (4)$$

where *PL* denotes the complex and *P* is the protein. The brackets indicate averages over MD trajectories, and due to stability issues,[40] all the averages are taken from a simulation of the complex. Each free energy is calculated as the sum of five terms

$$G = E_{\mathrm{vdW}} + E_{\mathrm{ele}} + \Delta G_{\mathrm{solv}} + \Delta G_{\mathrm{np}} + TS_{\mathrm{MM}} \qquad (5)$$

which are the molecular-mechanics (MM) van der Waals energy, the electrostatic energy, the polar solvation free energy, the non-polar solvation free energy, and the absolute temperature multiplied by an entropy estimated at the MM level, respectively. The polar solvation energy, was estimated with the generalised Born method of Onufriev et al., model I, i.e., with α = 0.8, β = 0, and γ = 2.91.[41] The non-polar solvation energy was estimated from the solvent-accessible surface area according to $\Delta G_{np} = \gamma \mathrm{SASA} + b$, where γ = 0.0227 kJ/mol/Å^2 and b = 3.85 kJ/mol. The entropy was estimated from harmonic frequencies, calculated at the MM level on a truncated and buffered system, as described previously, to improve the statistical precision of the estimate.[33] The other three terms were taken directly from the MD simulation, omitting the water molecules. All the terms in Eqn. 5 are averages over 40 snapshots taken from 40 independent MD simulations (i.e. in total 40 × 40 = 1600 energy estimates).[24] All MM/GBSA calculations were performed with the Amber 10 software.

Error estimates

All reported uncertainties are standard deviations of the mean (i.e. the standard deviation divided by the square root of the number of estimates). The standard error of the TI results was estimated in the following way: For each individual transformation and λ value, the standard deviation of the mean of $\partial V/\partial\lambda$ was calculated. Then, the standard deviation of the

total $\Delta\Delta G_{bind}$ estimate was obtained by error propagation (summing the variances, using the coefficients employed in the trapezoid formula). However, when several independent simulations were used to obtain the free energies (e.g. for ΔG_{conf}), the reported standard error is instead the standard deviation of the independent estimates divided by the square root of the number of independent calculations.

This latter approach was also used for the MM/GBSA estimates: The reported standard error is the standard deviation of the mean over the 40 independent simulations (ignoring the standard deviation among the 40 snapshots in each simulation).

The performance of the free energy estimates was quantified by the mean unsigned error (MUE) from the experimental data, the correlation coefficient between the predicted and experimental data (r^2), and Pearlman's predictive index (PI).[42] These estimates are quite meaningless without an estimate of their uncertainty. The standard deviation of these quality measures was obtain by a simple simulation approach:[24] Each inhibitor was assigned a random number from a Gaussian distribution, with the mean and standard deviation of the mean obtained from the TI or MM/GBSA calculations. The quality measures (MUE, r^2, and PI) were then calculated and the procedure was repeated 10 000 times. The standard error of these estimates is reported as the uncertainty.

MD simulations

All MD simulations were run using the sander module of Amber 10[38] or 11.[39] The temperature was kept constant at 300 K using a Langevin thermostat[43] with a collision frequency of 2.0 ps^{-1}, and the pressure was kept constant at 1 atm using a weak-coupling isotropic algorithm[44] with a relaxation time of 1 ps. Particle-mesh Ewald summation[45] with a fourth-order B spline interpolation and a tolerance of 10^{-5} was used to handle long-range electrostatics. The cut-off for non-bonded interactions was set to 8 Å and the non-bonded pair list was updated every 50 fs. The SHAKE algorithm[46] was used to constrain bonds involving hydrogen atoms so that a 2 fs time step could be used.

The TI simulations were performed in the following way: The system at each λ value was minimized for 500 cycles of steepest descent, with all atoms except water molecules and hydrogen atoms restrained to their start position with a force constant of 418 kJ/mol/$Å^2$. This was followed by a 20 ps constant-pressure simulation, using the same constraints, a 50 ps constant-pressure simulation without any restraints, and a 200 ps constant-volume simulation. Finally, a 2 ns production run was performed. The sampling frequency was determined by calculating the statistical inefficiency of the $\partial V/\partial\lambda$ estimates.[47] These calculations suggested that the correlation time was between 5 and 10 ps in different simulations. Therefore, a sampling time of 10 ps was used throughout this investigation.

The MD simulations for the MM/GBSA estimates basically followed the solvent-induced independent-trajectory (SIIT) approach recently suggested.[48] The 40 independent simulations were generated by solvating the protein–ligand complexes in different pre-equilibrated water boxes and using different random numbers for the initial velocities. The systems were then subjected to 500 cycles of steepest descent, with the same restraints as in the TI simulation, a 50 ps restrained constant-pressure simulation, followed by a 1 ns unrestrained constant-pressure simulations. Finally a 200 ps production run was performed and snapshots were saved every 5 ps.[24]

Results and Discussion

Relative free energies estimated by TI

We have carried out free energy calculation on a set of nine fXa inhibitors using the theoretical rigorous thermodynamic integration (TI) approach and the simpler MM/GBSA method. This allow for a direct comparison of the methods. However, first we will develop an optimal TI protocol for this system.

The relative free energies of the eight mutations in Figure 1, estimated by TI, are shown in Table 1. For five of the mutations, the TI estimates are within 1 kJ/mol of the experimental value[2] at least for one of the four combinations tested, TTA or STA and conformations A or B. In fact, for the **53**→**9** and **53**→**47** mutations all four methods give errors of less than 2 kJ/mol, and the same is true for conformation A for mutations **125**→**53** and **53**→**50**, whereas for mutation **53**→**59**, only TTA with the B conformation gives an error of 1 kJ/mol and the other methods give errors of 3–4 kJ/mol. These mutations also give a good precision of 0.6–0.8 kJ/mol for TTA and 0.3–0.7 kJ/mol for STA.

On the other hand, for three mutations, **63**→**39**, **53**→**57**, and **50**→**63**, the errors are instead 8–14 kJ/mol for all methods. All these mutations involve the amidinobenzyl group and they also involve all ligands with a single positive charge (i.e. mutations **53**→**57** and **50**→**63** involve a change of the net charge of the ligand, which has turned out to be problematic in previous TI studies[49]). The **63**→**39** mutation, on the other hand involves a H→OCH_3 mutation, i.e., the formation of a rather large group. However, similar large mutations have been carried out with higher accuracy previously.[50] The standard error for the free-energy estimates for the charge mutations is 1.4–1.7 kJ/mol, i.e. twice as large as for the five well-behaving mutations. Again STA gives a slightly better precision. The **63**→**39** mutation gives an intermediate precision of ~1 kJ/mol and the increased uncertainty comes mainly from the van der Waals perturbation (T2).

Simulation based on the two binding conformations (A and B) resulted in rather similar estimates for most of the mutations with differences of 0–6 kJ/mol. The largest differences are observed for the **53**→**50** and the **53**→**57** mutations. Neither of the two conformations gives consistently better results than the other.

Additional tests on some mutations

In an attempt to understand why three of the mutations give large errors compared to experiments, additional TI simulations based on the A conformation were carried out for these mutations.

For the **63**→**39** mutation, we performed three additional tests. First, we changed the TTA transformation scheme slightly: In the original scheme, T2 involves not only the van der Waals transformation, but also transformation of charges on atoms that are common to both ligands. If the van der Waals transformation is rather large, T2 may converge faster if we move all the charge transformations to T1 and T3 (i.e. if all charges in the ligand are zeroed in T1 and they are restored to those of ligand **39** in T3) and do only the van der Waals transformation in T2. Using this new scheme (which we call TTA' in the following), the estimated free energy was 0.4±3.0 kJ/mol. Thus, the error decreased from 12 to 10 kJ/mol, but the uncertainty increased by a factor of 2.5, so the change is not statistically significant. The larger uncertainty stems mainly from T1 and T3, because larger transformations are carried out. Therefore, ten independent MD simulations were carried out at each λ value. The use of independent trajectories has been shown to improve TI estimates for large mutations.[51] This resulted in an estimate of 0.4±4.9 kJ/mol, showing that the error estimate from error propagation underestimates the true uncertainty of the calculations. To improve the integration, more λ values were added at places where the curvature of the $\partial V/\partial\lambda$ curve was

high, but this did not result in any statistically significant change. Finally, ten independent TI calculations were carried out also with the original TTA decomposition and this resulted in an estimate of –3.5±1.2 kJ/mol, i.e. still no significant change.

For the **53**→**57** and **50**→**63** mutations, the alternative TTA' decomposition was also tested. The results were 11.0±2.5 kJ/mol and 20.7±2.7 kJ/mol, which are not significantly different from the original results. Further tests were carried out, but only on the first T1 transformation in the original TTA scheme, i.e. the removal of charges on atoms unique to ligands **53** and **50**, respectively. The number of λ values was increased to 19, the time step was reduced to 1 fs, the box size was doubled, the equilibration time was increased to 2.2 ns, and the production time was increased to 4 ns. The results of these tests are collected in Table 2. The only test that resulted in a significant improvement was the doubling of the box size for the **50**→**63** mutation. However, it is unclear if this is a general way to improve the results, because it did not lead to any significant improvement for the **53**→**57** mutation. However, the results show that these TI results are not fully converged with the standard protocol. In particular, it can be seen from Figure S1 (in the supplementary material) that the protein–ligand simulations require more than 2 ns to converge within 1 kJ/mol, whereas the free-ligand simulations are converged already after 1 ns.

Altogether, these test indicate that the poor results of the **63**→**39**, **53**→**57**, and **50**→**63**, mutations are not caused by convergence problems or limitations in the TI protocol used. Considering that all three mutations involve the same amidinobenzyl group, it is possible that the reason for the poor results is that these three ligands bind in a mode different from that observed in the crystal structure of ligand **125**. This is also supported by the fact that the two initial mutations of this group give a too positive energy difference, indicating that the final binding mode of ligands **57** and **63** is too unfavourable. We have tried to identify alternative binding modes for these ligands by MD simulations and docking, but we have not found any reasonable alternatives. Another possibility is that this amidinobenzyl group interacts with the surrounding protein through cation–π interactions with Trp and Phe groups and that this interaction is poorly described by the non-polarisable Amber force field.[52]

Free energy difference between A and B conformation

As mentioned in the Methods section, we also used TI to calculate the free energy difference of the binding energy for each ligand between conformations A and B, ΔG_{conf}. The results are shown in Table 3. All the free energy estimates were obtained from five independent simulations at each λ value. This was necessary in order to obtain a smooth curve for the integration, owing to the quite large changes during the transformations.

Starting with the TTA results, four of the ligands show a preference for the B conformation and the other five show a preference for the A conformation (by 0–6 kJ/mol). However, the uncertainties are so large for these estimates (2–3 kJ/mol), even though an independent-trajectory approach was used, so that none of the estimated ΔG_{conf} values is significantly different from 0 kJ/mol at the 95% confidence level. For ligand **125**, this is in line with the crystallographic data, which show equal occupancy of the two binding conformations. For the other ligands, these results indicate that the cleft where this part of the ligand binds is sufficiently large to accommodate two binding modes (see Figure 2).

The STA results predicts a preference for the B conformation for all ligands (by 1–11 kJ/ml), but again, none of the ΔG_{conf} estimates are significantly different from 0 kJ/mol. For seven of the ligands, the uncertainty is larger with the STA approach, compared to the TTA approach. This indicates that STA could have problems with larger mutations. On the other hand, only ligand **53** gives a significant difference between STA and TTA at the 95% confidence level.

Number of integration points

Considering that the results in Table 2 show no significant changes in the free energy when the number of integration points (λ values) is increased, it would be of interest to instead decrease the number of integration points, in order to decrease the computational expense. The free energy of charge transformations is usually assumed to follow the linear response approximation (LRA), according to which only two integration points are necessary to compute the free energy, viz. the end-points. We therefore calculated the difference $\Delta G_{bound} - \Delta G_{free}$ with only two λ values and compared the results with the estimates using all nine λ values using TTA. The results can be seen in Table 4 and most of the T1 and T3 transformations work well with only two λ values (0.1 and 0.9), with a mean absolute deviation (MAD) of less than 1 kJ/mol. However, three of the mutations showed larger differences, up to 3 kJ/mol. Moreover, the T2 transformation, which is mainly a van der Waals transformation, performed much worse, with a MAD of 2 kJ/mol and a maximum difference of 4 kJ/mol.

The use of two λ values implies a linear relation. Therefore, we also tested a single λ value (0.5). The results in Table 4 indicate that this extensive simplification gives slightly worse results than with two λ values, with MADs of 1 kJ/mol for T1 and T3, but 2 kJ/mol for T2, and with maximum deviations of up to 3 kJ/mol for T1 and 7 kJ/mol for T2.

Next, we computed the difference $\Delta G_{bound} - \Delta G_{free}$ with three (0.1, 0.5, and 0.9) and five (0.1, 0.3, 0.5, 0.7, and 0.9) λ values as well. These results are also shown in Table 4. It can be seen that at least five λ values are required if we aim at a MAD of less than 1 kJ/mol also for T2. The maximum difference is then less than 2 kJ/mol, which is actually similar to the standard error. Therefore, we tested two λ values for T1 and T3 and five λ values for T2, which will be denoted 2/5/2.

The difference in the total calculated binding free energies using 9 or 2/5/2 λ values are listed in Table 5. It can be seen that for four of the mutations, the difference is less than 1 kJ/mol, i.e. similar to the standard error. However, for the other four mutations, the deviation is larger, up to 6 kJ/mol. Still, the difference is statistically significant only for one of the sixteen mutations at the 95% level, viz., the **53**→**49** mutation in the B conformation. This deviation comes mainly from T3, which shows a deviation of –5.3 kJ/mol. This deviation is decreased to –1.2 kJ/mol if instead 3 λ values are used for T3. This indicates that it is safer to use 3/5/3 λ values instead. The results using such an approach are shown in Table 5 as well. It gives MADs and maximum deviations of less than 1 kJ/mol and 2–3 kJ/mol, respectively, which is more satisfying than the 2/5/2 results. The MUE of this approach compared to the experimental binding energies is slightly smaller than with nine λ values, but the difference is not significant.

Likewise, we also investigated how many λ values are necessary with STA. The results with one, two, three, and five λ values are compared with those with nine λ values in Table 4. It is clear that two λ values is not sufficient, giving a MAD of 2 kJ/mol and a maximum deviation of 8 kJ/mol. However, three λ values, seems to work surprisingly well with a MAD of less than 1 kJ/mol and a maximum difference of less than 3 kJ/mol. With five λ values, the MAD is 0.4 kJ/mol and the maximum deviation is 1 kJ/mol. Using three λ values, the calculated total binding free energies are shown in Table 5. It can be seen that that the MAD to the calculations with nine λ values is well below 1 kJ/mol, with maximum differences of 1–3 kJ/mol. In particular, none of the mutations gave any statistically significant difference. Compared to the experimental results, such an approach gives slightly larger errors (MUE = 6 kJ/mol) than with nine λ values, but the difference is not significant.

Simulation length

To further decrease the computational cost, the simulation length might be decreased. This is

especially pertinent to the protein–ligand simulations, because these have approximately five times larger CPU requirements than the free-ligand simulations. Therefore, we calculated $\Delta\Delta G_{bind}$ using 9 λ values, as a function of the protein–ligand simulation length for TTA. The results are plotted in Figure 4. If an error of 1 kJ/mol is accepted, all but the two simulations involving a change in the charge of the ligand have converged after 1 ns simulation. On the other hand, the charge mutations **53** → **57**, and **50** → **63** require 2.3–2.6 ns simulations to converge, as was discussed above (Figure S1). Thus, we can conclude that for mutations that do not involve a change of the total charge, the protein–ligand simulation length can be halved.

The next step is then to fix the protein–ligand simulation length at 1 ns, and evaluate $\Delta\Delta G_{bind}$ as a function of the length of the free-ligand simulation. This is shown in Figure 5. In this cases, the mutations **63** → **39**, **50** → **63**, and **125** → **53** show the slowest convergence, although the fluctuations are much smaller. If again an error of 1 kJ/mol is allowed, a 1.1 ns free-ligand simulation is needed.

If we repeat these evaluations, but using 3/5/3 λ values, the results are more or less the same as with using all the nine λ values (Figures S2 and S3), except that some of the free-ligand simulations show a slower convergence, up to 1.7 ns. Therefore, considering the relatively small gain of deceasing this simulation time from 2 to 1.1 ns, we suggest that a 2 ns free-ligand simulation is still motivated (and 1 ns for the protein–ligand simulations, unless the charge is changed). The results of such calculations are shown in Table 6. The MAD is 1 kJ/mol and the maximum deviation from the original approach is 5–6 kJ/mol. Only one of the charge mutations shows statistically significant changes. The standard errors of the $\Delta\Delta G_{bind}$ estimates are also shown in Table 6 and it can be seen that the precision is only slightly worse with this optimized protocol, 1 kJ/mol for the five well-behaving mutations, 2 kJ/mol for the two charge mutations, and ~1.5 kJ/mol for the **63** → **39** mutation. The MUE is not significantly different from the original results, 5 kJ/mol for the A conformation and 6 kJ/mol for the B conformation.

The same evaluation was repeated also for the STA. In Figures S4 and S5, $\Delta\Delta G_{bind}$ is plotted as a function of the length of the protein–ligand and free-ligand simulations, respectively. The results show that the former simulations are converged after 1 ns for all mutations, except the **50** → **63** charge mutation. Thus, the analysis showed that STA has the same equilibration properties as TTA. The results are similar when using only three integration points, as is shown in Figures S6 and S7. This implies that for most of the mutations, it is sufficient to use three λ values, 1 ns protein–ligand simulation time, and 2 ns free-ligand simulation time with STA. Again, the exceptions are mutations that involves a change of net charge. The results using such a protocol are collected in Table 6. It can be seen that it gives MADs of 1 kJ/mol and maximum deviations from the original scheme of 4–6 kJ/mol, although none of the differences are statistically significant. The precision is nearly identical to that of the TTA (3/5/3) protocol. The MUE compared to the experimental data is identical for the B conformation, but slightly larger for the A conformation (7 kJ/mol).

MM/GBSA estimates

MM/GBSA is a simpler method than TI, based on only end-point simulations of the protein–ligand complex. Therefore, it is interesting to compare the results of the two methods. In fact, MM/GBSA predicts absolute binding affinities. The absolute estimates for the binding of our nine fXa ligands are shown in Table 7. The MUEtr (the MUE when the mean signed error, –17 and –13 kJ/mol for conformation A and B, respectively, has been subtracted from each estimate) of 3–4 kJ/mol is impressive for this kind of calculation. However, it should be noted that the null-hypothesis that all the ligands have the same affinity gives a MUEtr of only 5 kJ/mol, so this good result mainly reflects the rather small range of binding affinities studied

(20 kJ/mol). On the other hand, the predictive index (PI) of the MM/GBSA estimates is 0.8, which shows that the ranking of the inhibitors is quite good, whereas the correlation coefficients of 0.7 and 0.5 are more mediocre.

Therefore, it would be interesting to compare the free energy differences for the eight considered mutations obtained with TI and MM/GBSA. The latter are also shown in Table 6. Interestingly, the MUEs of the MM/GBSA estimates, 4–5 kJ/mol, are actually somewhat lower than TI. This success of MM/GBSA can be attributed to the fact that it gives better results for the mutations involving a change of net charge (**53** → **57** and **50** → **63**), with errors of up to 6 kJ/mol. Instead, the largest error is found for the **63** → **39** perturbation (7–10 kJ/mol). On the other hand, the TI method gives a better correlation to the experimental results than MM/GBSA (r^2 = 0.3, compared to 0.2), although both correlations are quite poor. Likewise, MM/GBSA predicts the wrong sign of $\Delta\Delta G_{bind}$ for 3–4 of the eight mutations, whereas TI predicts the wrong sign for 2–3 of them.

The MM/GBSA calculations may also give some insight into the relative stability of the A and B conformations, because these estimates are based upon physically well-defined terms. The various energy terms for this difference are shown in Table 8. The electrostatic contribution ($\Delta E_{ele} + \Delta G_{solv}$) is small (< 2 kJ/mol) for most inhibitors, except for the ligands **49** and **57** (7 and 3 kJ/mol). The largest differences are instead found for the non-electrostatic part (up to 11 kJ/mol), which is typically dominated by the van der Waals term, although it is somewhat compensated by the entropy, i.e. an enthalpy–entropy compensation. It is interesting to note that MM/GBSA predicts that the A conformation is preferred for all of the ligands, contrary to TI (especially STA), which showed a slight preference for the B conformation. However, only one (TTA) or two (STA) of the differences are statistically significant at the 95% level.

The results MM/GBSA often depends strongly on the continuum-solvation method employed.[53] Therefore, we also tested the Poisson–Boltzmann solvation model, implemented in Amber 11. As can be seen in Table S1 in the supplementary material, such a MM/PBSA approach gave binding affinities that were 45 kJ/mol more positive on average than the corresponding MM/GBSA estimates. Unfortunately, these estimates reproduce the experimental results poorly, both in absolute and relative terms: In particular, both the correlation coefficient (r) and the PI are negative, indicating an anticorrelation for the absolute affinities. Likewise, the correlation coefficient is negative for the relative affinities. This shows that for this test case, there is no gain of using the more fundamental PB method than the GB method for continuum-solvation energies.

Finally, we also tested to calculate the affinities with a simple docking method, viz. AutoDock,[54] using default parameters and the AutoDock score function.[55] The protein was considered rigid in all docking calculations whereas the ligands were fully flexible. The results of these calculations are also included in Table S1 in the supplementary material. It can be seen that AutoDock also performed poor on this system: Both the correlation coefficient and the PI are negative for the absolute affinities. Likewise, the correlation coefficient is essentially zero for the relative affinities (r^2 = 0.02) and the MUE, 6 kJ/mol, is larger than for the null-hypothesis

Timings

When comparing the TI and MM/GBSA approaches, the time consumption of the two methods is of course also of interest. A 1-ns MD simulation of the protein–ligand complex takes ~34 CPU hours on a 2.27 GHz Intel Xeon machine, whereas the free-ligand simulations take only ~7 CPU hours. Moreover, the TI dual-topology implementation in Amber requires a minimum of 2 CPUs. From this we can estimate the total amount of CPU time required for the various protocols. These estimates are shown in Table 9. The original TTA protocol

requires in total ~4800 CPU hours, whereas the original STA protocol requires only ~1600 CPU hours. This is a huge amount, about 7 and 2 weeks, respectively, which is too expensive to use on a regular basis. If we instead use our optimised approach with a reduced number of integration points (3/5/3) and simulation lengths, the TTA approach takes ~1200 CPU hours, a 4-fold reduction. Likewise, the time-consumption for STA can be reduced by a factor of ~5 to 337 CPU hours. Moreover, the TI calculations can be trivially parallelised, by running the MD simulations at each integration point concurrently. Using such an approach, both TTA and STA take only ~40 CPU hours in the best scenario, but they then require at least 27 and 15 processors, respectively (two 2.2-ns free-ligand simulations can be run at the same time of one 1.2-ns protein–ligand complex simulation).

Surprisingly, the MM/GBSA estimates take ~1600 CPU hours, which is actually longer than for the optimised TI approaches. The reason for this is that the inherent precision is better for TI, because it calculates only relative energies, whereas MM/GBSA always calculates absolute binding energies. Therefore, MM/GBSA requires a large number of independent simulations (40) to obtain a precision of 1 kJ/mol. Of course, the time consumption of MM/GBSA can be strongly reduced if a lower precision is tolerated (e.g. by a factor of 4 for a precision of 2 kJ/mol), but the same applies to TI and it is quite meaningless to compare methods that do not give a similar precision (the precision of the MM/GBSA estimates are already slightly worse than that of TI). Moreover, fXa requires a long equilibration time with the SIIT approach. A gain in total CPU time could be obtained if the velocity-induced independent trajectories (VIIT) approach was instead used to generate the independent simulations,[48] because this would allow the long equilibration (1 ns) to be run only once (total CPU time ~540 h, i.e. still longer than for the optimised STA approach). To this we should add a few hours of post-processing, (TI requires only a couple of minutes for the integration). On the other hand, MM/GBSA could gain from using the pmemd module in Amber, which is significantly faster (by a factor of ~2) than the standard sander module, especially in parallel runs, but it cannot be used for TI. If all calculations could be run concurrently, the MM/GBSA SIIT approach would require 40 CPU h on 40 nodes. The 40 bulk calculations with the VIIT approach would take only 17 CPU h, but a single 1 ns equilibration (34 h) would probably still be required.

Conclusions

We have calculated binding free-energy differences for eight pairs of fXa 3-amidinobenzyl-1*H*-indole-2-carboxamide inhibitors with the TI and MM/GBSA methods. This turned out to be quite difficult, because the ligands can bind in two distinct conformations. Therefore, we estimated the free energy of mutating conformation A to B for each ligand bound to the protein. Unfortunately, these mutations are hard to converge, but the results indicate that neither conformation is significantly preferred over the other, in accordance with the crystal structure showing equal occupancy for the two conformations of ligand **125**.[2]

With a standard TI protocol, we could estimate the difference in binding free energy of five pairs of ligands with a precision better than 1 kJ/mol and with a MUE of 2 kJ/mol. The STA protocol (with a single transformation at each λ value), gave a slightly better precision and it is appreciably faster and simpler . For two mutations that involved a change of the net charge of the ligand, the statistical uncertainty was twice as large and the errors 7–14 kJ/mol. For the last mutation (**63**→**39**), the precision was intermediate, but the error was still large. This may indicate that ligands with neutralising mutations in the amidinobenzyl group binds in a different mode.

Encouragingly, we have shown that for most of the mutations, the TI protocol can be tuned to decrease the computational demand while still retaining the accuracy and precision. If all simulations at each λ values can be run concurrently, one could obtain an TI estimate of

ΔG_{bind} within ~2 days (on 15–27 CPUs) and both the TTA and STA approaches take a same amount of time, whereas STA is better if one has more limited computer resources.

Quite unexpectedly, we found that the more approximate MM/GBSA method gives overall estimates that are somewhat better than the TI results. However, this is mainly owing to that MM/GBSA performs better for the mutations that involve a change of the net charge. Interestingly, in its current implementation, the MM/GBSA method has a larger total computational demand than TI, if a similar precision is required for both methods.

In conclusion, our results indicate that TI could be a useful tool in drug design with a carefully design the simulations, if all ligands involve a common scaffold. Mutations that change the charge should be avoided, because they are prone give to large errors and are much harder to converge. Without such mutations, we have shown that a precision better than 1 kJ/mol and a average accuracy of 2 kJ/mol could be obtained at a cost of ~340 CPU h per ligand.

Acknowledgements
This investigation has been supported by grants from the Swedish research council (project 2006-4417) and from the Research school in pharmaceutical science. It has also been supported by computer resources of Lunarc at Lund University, C3SE at Chalmers University of Technology and HPC2N at Umeå University.

1 Rai, R.; Sprengeler, P. A.; Elrod, K. C.; Young, W. B. Perspectives on Factor Xa Inhibition. *Curr. Med. Chem.* **2001**, *8*, 101-119.

2 Matter, H.; Defossa, E.; Heinelt, U.; Blohm, P.-M.; Schneider, D.; Müller, A.; Hreok, S. I.; Schreuder, H.; Liesum, A.; Brachvogel, V.; Lönze, P.; Walser, A.; Al-Obeidi, F.; Wildgoose, P. Design and quantitative structure-activity relationship of 3-amidinobenzyl-1H-indole-2-carboxamides as potent, nonchiral, and selective Inhibitors of blood coagulation factor Xa. *J. Med. Chem.* **2002**, *45*, 2749-2769.

3 Ostrosky, D.; Udier-Blagovic, M.; Jorgensen, W. L. Analyses of Activity for Factor Xa Inhibitors Based on Monte Carlo Simulations. *J. Med. Chem.* **2003**, *46*, 5691-5699

4 Taha, M. O.; Qandil, A. M.; Zaki, D. D.; AlDamen, M. A. Ligand-based assessment of factor Xa binding site flexibility via elaborate pharmacophore exploration and genetic algorithm-based QSAR modeling. *Eur. J. Med. Chem.* **2005**, *40*, 701-727.

5 Davie, E. W.; Fujikawa, K.; Kisiel, W. The coagulation cascade: initiation, maintenance, and regulation. *Biochemistry* **1991**, *30*, 10363-10370.

6 Garcia, D.; Libby, E.; Crowther, M. A. The new oral anticoagulants. *Blood*, **2010**, *115*, 15-20.

7 Eikelboom, J. W.; Weitz, J. I. Update on Antithrombotic Therapy. New Anticoagulants. *Circulation*, **2010**, *121*, 1523-1532.

8 Gohlke, H.; Klebe, G. Approaches to the description and prediction of the binding affinity of small-molecule ligands to macromolecular receptors. *Angew. Chem. Int. Ed.* **2002**, *41*, 2644-2676.

9 Kirkwood, J. G. Statistical mechanics of fluid mixtures. *J. Chem. Phys.* **1935**, *3*, 300-313.

10 Fujitani, H.; Tanida, Y.; Ito, M.; Jayachandran G.; Snow, C. D.; Shirts, M. R.; Sorin, E. J.; Pande, V. S. Direct calculation of the binding free energies of FKBP ligands. *J. Chem. Phys.* **2005**, *123*, 084108.

11 Chipot, C.; Rozanska, X.; Dixit, S. B. Can free energy calculations be fast and accurate at the same time? Binding of low-affinity, non-peptide inhibitors to the SH2 domain of the src protein. *J. Comput. Aided Mol. Design.* **2005**, *19*, 765-770.

12 Sham, Y. Y.; Chu, Z. T.; Tao, H.; Warshel, A. Examining methods for calculations of binding free energies: LRA, LIE, PDLD-LRA, and PDLD/S-LRA calculations of ligands binding to an HIV protease. *Proteins: Struct Funct Genet* **2000**, *39*, 393-407.
13 Åqvist, J.; Medina, C.; Samuelsson, J. E. A new method for predicting binding affinity in computer-aided drug design. *Prot. Eng.* **1994**, *7*, 385-391.
14 Srinivasan, J.; Cheatham III, T. E.; Cieplak, P.; Kollman, P. A.; Case, D. A. Continuum Solvent Studies of the Stability of DNA, RNA, and Phosphoramidate−DNA Helices. *J. Am. Chem. Soc.* **1998**, *120*, 9401-9809.
15 Kollman, P.; A.; Massova, I.; Reyes, C.; Kuhn, B.; Huo, S.; Chong, L.; Lee, M.; Lee, T.; Duan, Y.; Wang, W.; Donini, O, Cieplak, P.; Srinivasan, J.; Case, D. A.; Cheatham III, T.; E. Calculating structures and free energies of complex molecules: Combining molecular mechanics and continuum models. *Acc. Chem. Res.* **2000**, *33*, 889-897.
16 Hu, G.; Wang, D.; Liu, X.; Zhang, A. A computational analysis of the binding model of MDM2 with inhibitors. *J. Comput. Aided Mol. Des.* **2010**, *24*, 687-697.
17 Stoica, I.; Sadiq, S. K.; Coveney, P. V. Rapid and accurate prediction of binding free energies for saquinavir-bound HIV-1 proteases. *J. Am. Chem.* Soc. **2008**, *130*, 2639-2648.
18 Gohlke, H.; Case, D. A. Converging free energy estimates: MM-PB(GB)SA studies on the protein-protein complex ras-raf. *J Comput. Chem.* **2003**, *25*, 238-250.
19 Sadiq, S. K.; Wright, D. W.; Kenway, O. A.; Coveney, P. V. Accurate ensemble molecular dynamics binding free energy ranking of multidrug-resistant HIV-1 proteases. *J. Chem. Inf. Model.* **2010**, *50*, 890-905.
20 Pearlman, D. A. Evaluating the molecular mechanics Poisson-Boltzmann surface area free energy method using a congeneric series of ligands to p38 MAP kinase. *J. Med. Chem.* **2005**, *48*, 7796-7807.
21 Kuhn, B.; Greber, P.; Schulz-Gasch, T.; Stahl, M.Validation and use of the MM-PBSA approach for drug discovery. *J. Med. Chem.* **2005**, *48*, 4040-4048.
22 Weis, A.; Katebzadeh, K.; Söderhjelm, P.; Nilsson, I.; Ryde U. Ligand affinities predicted with the MM/PBSA method: dependence on the simulation method and the force field. J. Med. Chem. 2006, 49, 6596-6606.
23 Kongsted, J.; Ryde, U. An improved method to predict the entropy term with the MM/PBSA approach. *J. Comput-Aided Mol. Design.* **2009**, *23*, 63-71.
24 Genheden, S.; Ryde, U. How to obtain statistically converged MM/GBSA results. *J. Comput Chem.* **2010**, *31*, 837-846.
25 Oostenbrink, C.; van Gunsteren, W. F. Single-step perturbations to calculate free energy differences from unphysical reference states: limits on size, flexibility, and character. *J. Comput. Chem.* **2003**, *24*, 1730-1739.
26 Villa, A.; Zangi, R.; Pieffet, G.; Mark, A. E. Sampling and convergence in free energy calculations of protein-ligand interactions: The binding of triphenoxypyridine derivatives to factor Xa and trypsin. *J. Comput. Aided Mol. Des.* **2003**, *17*, 673-686.
27 Huang, D.; Cafisch, A. Efficient evaluation of binding free energy using continuum electrostatics solvation. *J. Med. Chem.* **2004**, *45*, 5791-5797.
28 Rao, M. S.; Olson, A. J. Modelling of factor Xa-inhibitor complexes: A computational flexible docking approach. *Proteins* **1999**, *34*, 173-183.
29 Murcia, M.; Ortiz, A. R. Virtual screening with flexible docking and combine-based models. Application to a series of factor Xa inhibitors. *J. Med. Chem.* **2004**, *47*, 805-820.
30 Ewing, T. J. A.; Makino, S.; Skillman, A. G.; Kuntz, I. D. DOCK 4.0: Search strategies for

automated molecular docking of flexible molecule databases. *J. Comput. Aided Mol. Des.* **2001**, *15*, 411-428.

31 Cornell, W. D.; Cieplak, P.; Bayly, C. I.; Gould, I. R.; Merz, K. M.; Ferguson, D. M.; Spellmeyer, D. C.; Fox, T.; Caldwell, J. W.; Kollman, P. A. A second generation force field for the simulation of proteins, nucleic acids, and organic molecules. *J. Am. Chem Soc.* **1995**, *117*, 5179-5197.

32 Wang, J. M.; Wolf, R. M.; Caldwell, K. W.; Kollman, P. A.; Case, D. A. Development and testing of a general Amber force field. *J. Comput. Chem.* **2004**, *25*, 1157-1174

33 Bayly, C. I.; Cieplak, P.; Cornell, W. D.; Kollman, P. A. A well-behaved electrostatic potential based method using charge restraints for deriving atomic charges: the RESP model. *J. Phys. Chem.* **1993**, *97*, 10269-10280.

34 Besler, B. H.; Merz, K. M.; Kollman, P. A. Atomic charges derived from semiempirical methods. *J. Comput. Chem.* **1990**, *11*, 431-439.

35 Jorgensen, W. L.; Chandrasekhar, J.; Madura, J. D.; Impley, R. W.; Klein, M. L. Comparison of simple potential functions for simulating liquid water. *J. Chem. Phys.* **1983**, *79*, 926-935.

36 Steinbrecher, T.; Mobley, D. L.; Case, D. A. Nonlinear scaling schemes for Lennard-Jones interactions in free energy calculations. *J. Chem. Phys.* **2007**, *127*, 214108.

37 Michel, J.; Essex, J. W. Prediction of protein–ligand binding affinity by free energy simulations: assumptions, pitfalls and expectations. *J. Comput. Aided Mol. Des.* **2010**, *24*, 639-658.

38 Case, D. A.; Darden, T. A.; Cheatham III, T. E.; Simmerling, C. L.; Wang, J.; Duke, R. E.; Luo, R.; Crowley, M.; Walker, R.; C.; Zhang, W.; Merz, K. M.; Wang, B.; Hayik, S.; Roitberg, A.; Seabra, G.; Kolossvary, I.; Wong, K.; F.; Paesani, F.; Vanicek, J.; Wu, X.; Brozell, S. R.; Steinbrecher, T.; Gohlke, H.; Yang, L.; Tan, C.; Mongan, J.; Hornak, V.; Cui, G.; Mathews, D. H.; Seetin, M. G.; Sagui, C.; Babin, V.; Kollman, P. A. Amber 10, University of California, San Francisco, **2008**.

39 Case, D.A.; Darden, T.A. , Cheatham, III, T.E.; Simmerling, C.L.; Wang, J. Duke, R.E.; Luo, R.; Walker, R.C.; Zhang, W.; Merz, K.M.; Roberts, B.; Wang, B.; Hayik, S.; Roitberg, A.; Seabra, G.; Kolossváry, I.; Wong, K.F.; Paesani, F.; Vanicek, J.; Wu, X.; Brozell, S.R.; Steinbrecher, T.; Gohlke, H.; Cai, Q.; Ye, X.; Wang, J.; Hsieh, M.-J.; Cui, G.; Roe, D.R.; Mathews, D.H.; Seetin, M.G.; Sagui, C.; Babin, V.; Luchko, T.; Gusarov, S.; Kovalenko, A.; Kollman P.A. AMBER 11, University of California, San Francisco, **2010**.

40 Swanson, J. M. J.; Henchman, R. H.; McCammon, J. A. Revisiting Free Energy Calculations: A Theoretical Connection to MM/PBSA and Direct Calculation of the Association Free Energy. *Biophys. J.* **2004**, *86*, 67-74.

41 Onufriev, A.; Bashford, D.; Case, D. A. Exploring protein native states and large-scale conformational changes with a modified generalized Born model. *Proteins* **2004**, *55*, 383-394.

42 Pearlman, D. A.; Charifson, P. S. Are free energy calculations useful in practice? A comparison with rapid scoring functions for the p38 map kinase protein system. *J. Med. Chem.* **2001**, *44*, 3417-3423.

43 Wu, X.; Brooks, B. R. Self-guided Langevin dynamics simulation method. *Chem. Phys. Lett.* **2003**, *381*, 512-518.

44 Berendsen, H. J. C.; Postma, J. P. M.; van Gunsteren, W. F.; DiNola, A.; Haak, J. R. Molecular dynamics with coupling to an external bath. *J. Chem. Phys.* **1984**, *81*, 3684–

3690.
45 Darden, T.; York, D.; Pedersen, L. Particle mesh Ewald: An $N\cdot\log(N)$ method for Ewald sums in large systems. *J. Chem. Phys.* **1993**, *98*, 10089-10092.
46 Ryckaert, J. P.; Ciccotti, G.; Berendsen, H. J. C. Numerical integration of the Cartesian equations of motion of a system with constraints: Molecular dynamics of *n*-alkanes. *J. Comput. Phys.* **1977**, *23*, 327-341.
47 Yang, W.; Bitetti-Putzer, R.; Karplus, M. Free energy simulations: Use of reverse cumulative averaging to determine the equilibrated region and the time required for convergence. *J. Chem. Phys.* **2004**, *120*, 2618-2628.
48 Genheden S.; Ryde, U. A comparison of different initialisation protocols to obtain statistically independent molecular dynamics simulations. *J. Comput. Chem.* **2011***, 32*, 187-195.
49 Steinbrecher, T.; Case, D. A.; Labahn, A. A multistep approach to structure-based drug design: Studying ligand binding at the human neutrophil elastase. *J. Med. Chem.* **2006**, *49*, 1837-1844.
50 Michel, J.; Verdonk, M. L.; Essex, J. Protein-ligand binding affinity predictions by implicit solvent simulations: A tool for lead optimization? *J. Med. Chem.* **2006**, *49*, 7427-7539.
51 Lawrenz, M.; Baron, R.; McCammon, J. A. *J. Chem. Theory Comput.* 2009, *5*, 1106-1116.
52 Caldwell, J. W.; Kollman, P. A. Cation-π interactions: nonadditive effects are
critical in their accurate representation. *J. Am. Chem. Soc.* **1995**, *117*, 4177-4178.
53 Genheden, S.; Luchko, T.; Gusarov, S.; Kovalenko, A.; Ryde, U. An MM/3D-RISM approach for ligand-binding affinities. *J. Phys. Chem. B.* **2010**, *114*, 8505-8516.
54 Morris, G. M.; Goodsell, D. S.; Halliday, R.S.; Huey, R.; Hart, W. E.; Belew, R. K.; Olson, A. J. Automated docking using a Lamarckian genetic algorithm and an empirical binding free energy function. *J. Comp. Chem*. **1998**, *19*, 1639-1662.
55 Huey, R.; Morris, G. M.; Olson, A. J.; Goodsell, D. S. A semiempirical free energy force field with charge-based desolvation. *J. Comp. Chem*. **2007**, *28*, 1145-1152.

Table 1. Free energy differences estimated by TI (kJ/mol).

	A conformation		B conformation		Difference [a]		
Mutation	TTA	STA	TTA	STA	TTA	STA	Exp
125 → 53	-1.3±0.9	-2.4±0.4	0.9±0.8	1.8±0.3	2.2	-4.2	-1.0
53 → 9	-0.2±0.7	-1.2±0.5	-1.1±0.7	-0.9±0.5	-0.9	-0.3	-1.9
53 → 47	-0.7±0.6	-1.1±0.5	-0.9±0.6	-0.9±0.5	-0.1	-0.2	-2.5
53 → 49	-1.6±0.8	-1.8±0.6	1.3±0.8	-1.0±0.6	2.8	-0.8	2.5
53 → 50	-0.9±0.8	-0.2±0.7	-7.0±0.8	-5.3±0.7	-6.1	5.1	-1.9
53 → 57	14.9±1.6	17.5±1.4	20.0±1.5	13.8±1.4	5.1	3.7	6.3
50 → 63	20.1±1.7	19.2±1.5	16.0±1.5	18.5±1.4	-4.2	0.7	8.8
63 → 39	-2.0±1.2	-4.0±0.8	-2.9±1.2	-3.6±1.0	-1.0	-0.3	10.1
MUE [b]	5.1±0.4	5.6±0.3	5.6±0.4	5.4±0.3			
Max [c]	12.0	14.0	13.7	13.7			
r^2	0.33±0.04	0.27±0.03	0.31±0.04	0.29±0.07			

[a] Difference in ΔG_{bind} between A and B conformations.
[b] Mean unsigned error from experimental results.
[c] Maximum error from experimental results.
[d] Experimental results.[2]

Table 2. T1 free energy differences from additional tests on two mutations (kJ/mol).

Mutation	Original	19 λ values	1 fs time step	Doubled box size	2.2 ns equilibration	4 ns production
53 → 57	17.8±1.4	17.7±1.4	17.6±1.4	16.2±1.4	14.3±1.3	16.0±1.0
50 → 63	20.0±1.4	20.9±1.4	17.9±1.5	13.4±1.4	25.0±1.3	21.8±1.1

Table 3. Free energy difference between the two binding conformations of each ligand (ΔG_{conf} ; kJ/mol).

Ligand	TTA	STA
9	0.6±3.0	-11.2±4.9
39	-2.5±2.1	-0.8±1.6
47	-6.2±3.1	-7.8±6.2
49	-4.4±2.6	-8.5±5.5
50	1.9±2.8	-8.4±5.1
53	5.3±2.4	-6.7±3.7
57	-0.7±2.5	-6.8±3.3
63	0.3±1.4	-0.5±1.2
125	0.9±2.6	-5.5±3.9

Table 4. Relative free energy estimates with varying number of λ values (kJ/mol).

	T1				T2				T3				STA			
# λ values	1	2	3	5	1	2	3	5	1	2	3	5	1	2	3	5
125 → 53	2.6	-0.3	0.8	0.6	0.3	-0.4	-0.1	0.1	1.3	0.2	0.6	0.2	1.7	-1.4	-0.2	0.4
53 → 9	1.3	0.3	0.7	0.2	-0.6	-0.8	-0.7	-0.5	-0.1	0.0	0.0	0.0	0.5	-1.2	-0.6	-0.2
53 → 47	0.4	0.0	0.2	-0.2	-2.2	1.8	0.3	-0.1	0.2	0.0	0.1	0.0	-0.4	-1.4	-0.2	0.4
53 → 49	0.1	0.1	0.1	0.1	-4.5	3.8	0.7	0.0	2.1	-2.7	-0.9	-0.9	1.1	-0.3	0.2	0.8
53 → 50	0.5	0.2	0.3	0.2	0.4	0.6	0.5	0.2	-0.8	0.4	-0.1	0.1	-0.8	0.1	-0.2	-0.3
53 → 57	-3.2	3.0	0.6	0.1	0.0	-0.3	-0.2	0.3	-1.7	-0.2	-0.7	-0.3	-6.5	-0.3	-2.6	0.3
50 → 63	-0.8	2.3	1.1	-0.1	-1.5	3.5	1.6	1.2	-0.8	0.3	-0.1	-0.2	-11.2	7.9	0.7	-0.1
63 → 39	0.6	-0.4	0.0	0.0	7.1	4.2	5.3	1.6	-0.8	0.9	0.3	-0.2	-4.4	4.8	1.4	1.0
MAD	1.2	0.8	0.5	0.2	2.1	1.9	1.2	0.5	1.0	0.6	0.3	0.2	3.3	2.2	0.8	0.4
Max	3.2	3.0	1.1	0.6	7.1	4.2	5.3	1.6	2.1	-2.7	0.6	0.2	11.2	7.9	2.6	1.0

All free energies are deviations from the estimate using nine λ values. A positive error indicates that the estimate with nine λ values is more positive. The five λ values were 0.1, 0.3, 0.5, 0.7 and 0.9, the three λ values were 0.3, 0.5 and 0.9, the two λ values were 0.1 and 0.9, whereas the single λ value was 0.5. The A conformation was considered in all calculations. MAD and Max are the mean absolute deviation and maximum deviation from the estimate with nine λ values.

Table 5. Free energies differences estimated using fewer λ values (kJ/mol).

	A conformation			B conformation		
Mutation	TTA (2/5/2)	TTA (3/5/3)	STA (3)	TTA (2/5/2)	TTA (3/5/3)	STA (3)
125 → 53	-0.2	1.5	0.4	0.3	0.1	-0.1
53 → 9	-0.2	0.1	-0.2	-0.6	-1.1	-0.9
53 → 47	0.0	0.2	0.1	-0.3	-0.2	-0.2
53 → 49	-2.6	-0.8	0.8	-5.6*	-1.3	-1.1
53 → 50	0.8	0.5	-0.3	1.1	0.5	0.5
53 → 57	2.6	0.2	0.3	4.7	2.9	-1.5
50 → 63	3.8	2.2	-0.1	-3.2	-1.0	1.2
63 → 39	2.1	1.8	1.0	-1.1	0.0	2.6
MAD	1.5	0.8	0.3	2.1	0.8	0.9
Max	3.8	2.2	1.0	5.6	2.9	2.6
MUE	4.1±0.4	5.0±0.4	6.1±0.3	5.9±0.4	5.4±0.3	5.8±0.4

The table reports differences relative to the results obtained with nine λ values. A positive difference indicates that the estimate with nine λ values is more positive. The number of λ values used is indicated in the parenthesis. * marks deviations that are statistically significant at the 95% level. MAD and Max are the mean absolute deviation and maximum deviation from the estimate with nine λ values. MUE is the mean unsigned error compared to the experimental data.

Table 6. Free energies estimated using shorter simulation time (kJ/mol).

	A conformation		B conformation	
Mutation	TTA (3/5/3)	STA (3)	TTA (3/5/3)	STA (3)
125 → 53	-2.7±1.1	-2.1±1.1	-0.1±1.0	2.0±1.0
53 → 9	0.3±0.9	-0.7±0.9	0.8±0.9	0.6±0.9
53 → 47	-0.8±0.8	-1.4±0.8	-0.3±0.8	-0.7±0.8
53 → 49	1.3±1.0	-1.4±1.0	2.8±1.0	0.3±1.0
53 → 50	-2.4±1.0	0.3±1.0	-8.2±1.0	-5.6±1.1
53 → 57	20.4±1.9**	22.5±1.9	21.9±2.1	14.6±2.1
50 → 63	14.1±2.1	24.3±2.1	17.9±2.0	13.6±2.1
63 → 39	-4.1±1.5	-4.9±1.4	-3.4±1.6	-7.0±1.5
MAD	1.5	1.1	1.0	0.7
Max	5.7	5.9	4.8	3.7
MUE	5.1±0.5	7.0±0.5	6.3±0.5	5.4±0.5

The length of the production simulation was 1 ns for the protein–ligand simulation and 2 ns for the free-ligand simulations. The number of λ values is shown in parenthesis. ** marks deviations from a protein–ligand simulation length of 2 ns that are statistically significant at the 99% level.

Table 7 – MM/GBSA free energies (kJ/mol).

Ligand	A conformation	B conformation	Exp.
9	-65.5±0.9	-65.5±1.6	-46.2
39	-49.4±0.9	-48.0±1.4	-27.3
47	-58.8±1.1	-55.7±1.3	-46.8
49	-59.4±1.0	-59.2±2.1	-41.9
50	-57.8±0.8	-53.4±1.6	-46.2
53	-62.5±1.0	-57.7±1.8	-44.3
57	-57.2±1.2	-49.4±1.1	-38.0
63	-52.2±1.6	-48.1±1.4	-37.4
125	-63.4±1.0	-57.7±1.2	-43.4
MUEtr	2.9±0.3	3.7±0.5	
r^2	0.67±0.06	0.50±0.09	
PI	0.83±0.06	0.79±0.07	
Mutation	A conformation	B conformation	Exp.
125 → 53	0.9±1.4	0.0±1.7	-1.0
53 → 9	-3.0±1.4	-7.7±1.9	-1.9
53 → 47	3.7±1.5	2.0±1.8	-2.5
53 → 49	3.1±1.4	-1.5±2.0	2.5
53 → 50	4.7±1.4	4.3±1.9	-1.9
53 → 57	5.3±1.5	8.3±1.7	6.3
50 → 63	5.6±1.6	5.3±1.7	8.8
63 → 39	2.8±1.6	0.1±1.7	10.1
MUE	3.5±0.5	4.6±0.6	
r^2	0.24±0.1	0.16±0.1	

Table 8 – MM/GBSA energy terms for the difference in binding energy between the A and B conformations (kJ/mol).

Ligand	E_{ele}	E_{vdW}	ΔG_{solv}	ΔG_{np}	$-T\Delta S_{MM}$	$E_{ele}+\Delta G_{solv}$	$E_{vdW}+\Delta G_{np}-T\Delta S_{MM}$	ΔG_{conf}
9	44.2	7.1	-45.7	0.4	-6.0	-1.5	1.6	0.1
39	-5.5	-1.1	7.4	0.0	0.6	1.8	-0.5	1.4
47	57.8	9.5	-59.3	0.4	-5.4	-1.5	4.6	3.1
49	33.7	9.2	-40.8	0.4	-2.3	-7.0	7.3	0.2
50	49.6	9.2	-49.8	0.4	-5.0	-0.2	4.6	4.4
53	57.4	11.0	-59.3	0.5	-4.8	-1.9	6.7	4.8
57	12.9	13.6	-16.2	1.0	-3.6	-3.2	11.0	7.8
63	7.6	4.7	-8.1	0.3	-0.4	-0.6	4.6	4.1
125	73.3	9.0	-73.8	0.5	-3.3	-0.5	6.2	5.7

Table 9 – CPU timings of the various approaches.

Approach	λ values	Protein–ligand simulation (ns)	Total time (CPUh)	Total parallel time (CPUh)[b]
TTA	9	2.2	4846	74
TTA	3/5/3	1.2	1236	40
STA	9	2.2	1615	74
STA	3	1.2	337	40
MM/GBSA, SIIT	40[a]	1.2	1610	40
MM/GBSA, VIIT	40[a]	1.0+0.4	564	47

[a] Number of independent simulations
[b] If the simulations at each integration point are run concurrently.

Figure 1 – The nine fXa inhibitors considered in this study. The mutations explicitly modelled in the TI calculations are shown with arrows, and the groups introduced in each mutation are shown in bold.

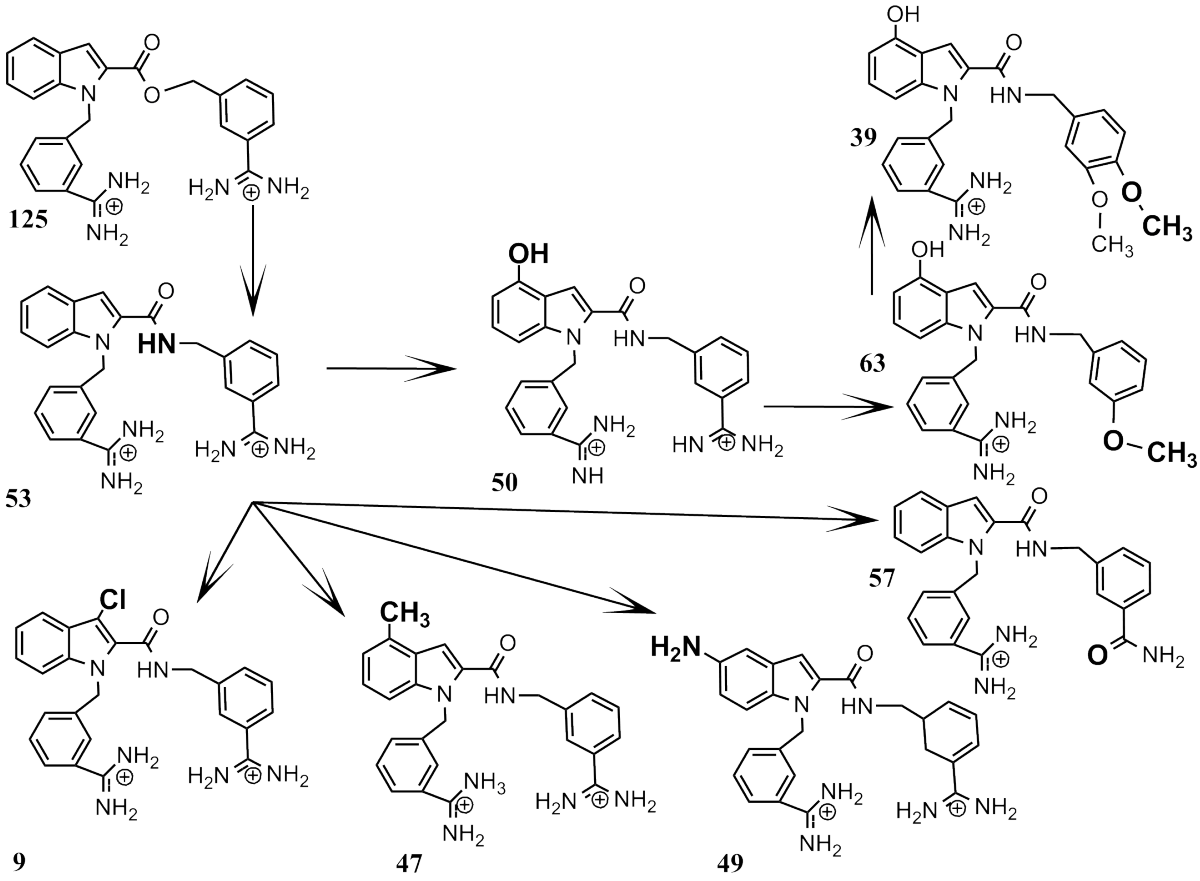

Figure 2 – The two conformations of ligand 125 in the crystal structure.[2] The A conformation is shown in cyan and the B conformation is shown in green (without non-polar hydrogen atoms).

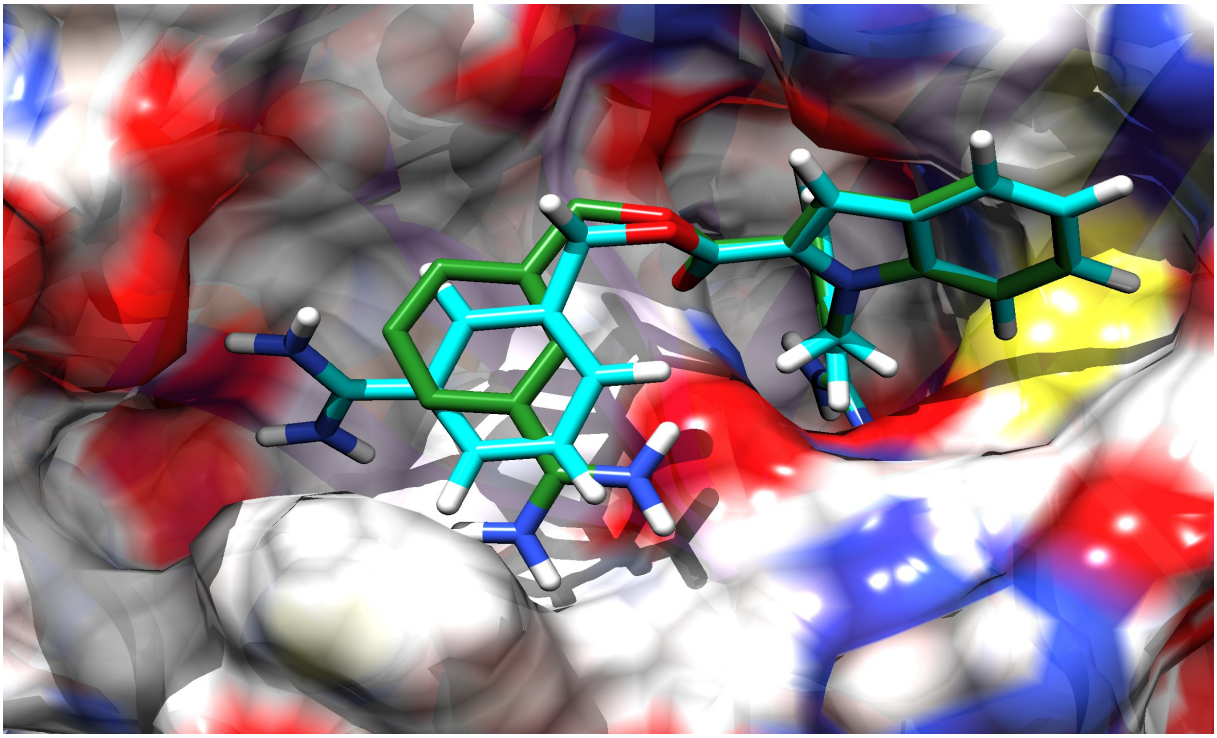

Figure 3 – The thermodynamic cycle used to compute the free energy differences.

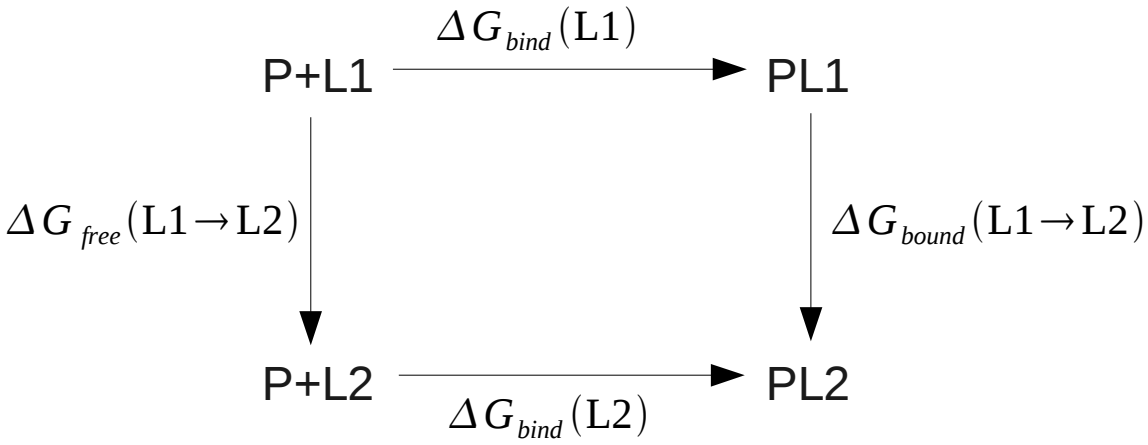

Figure 4 – The dependence of $\Delta\Delta G_{bind}$ on the protein–ligand simulation length for the TTA approach. The free energies shown are deviations relative to a simulation time of 2 ns.

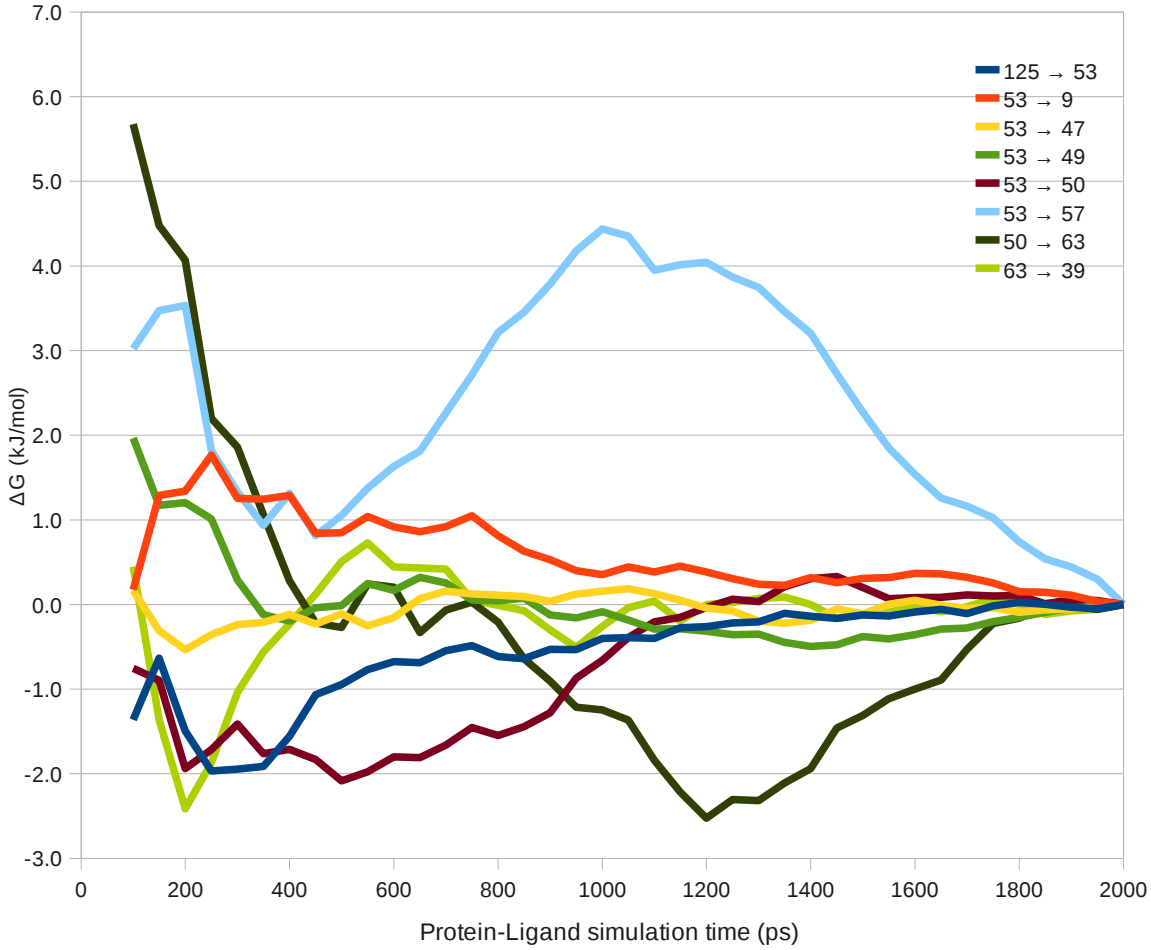

Figure 5 – The dependence of $\blacktriangle\blacktriangle G_{bind}$ on the free-ligand simulation length with the TTA approach. The free energies shown are deviations relative to a simulation time of 2 ns. The protein–ligand simulation time was fixed at 1 ns.

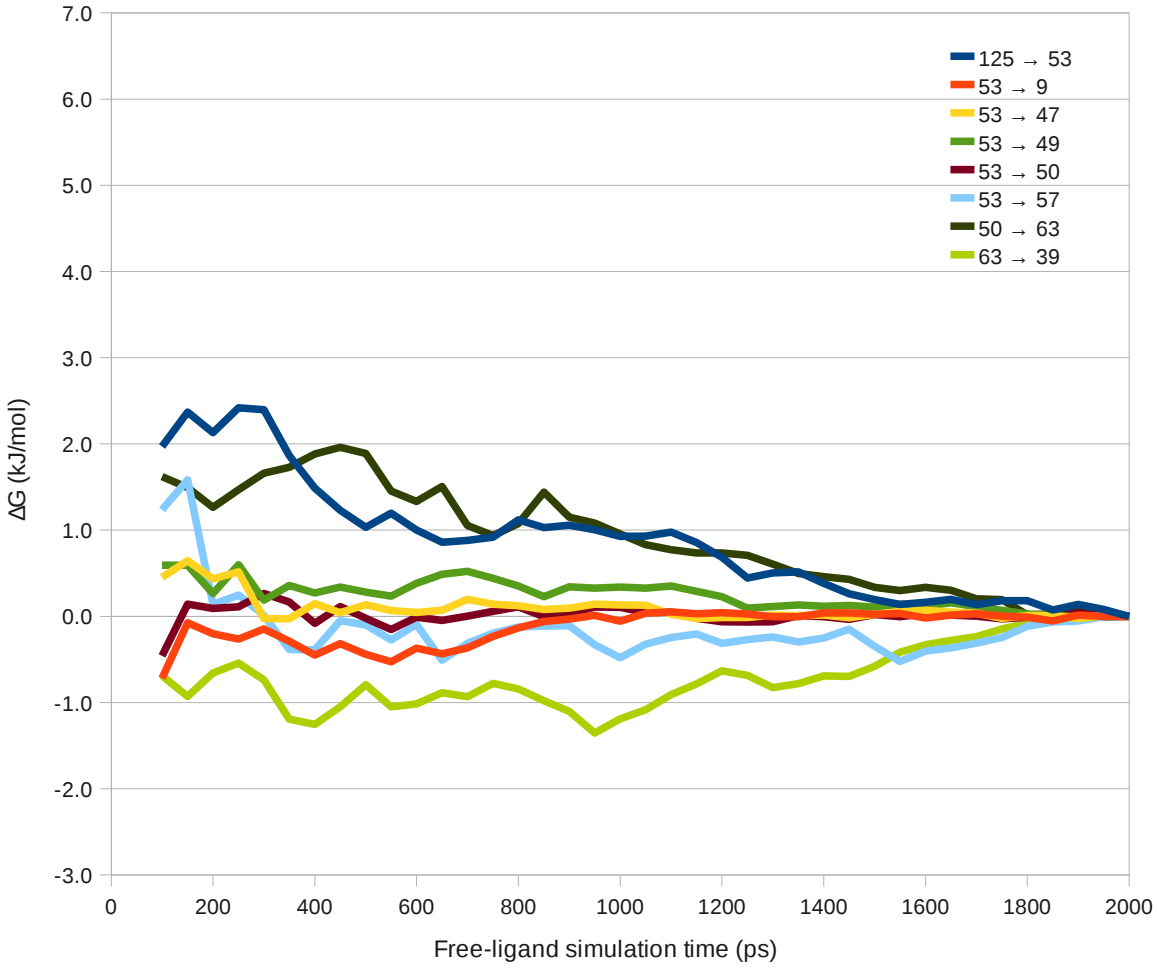
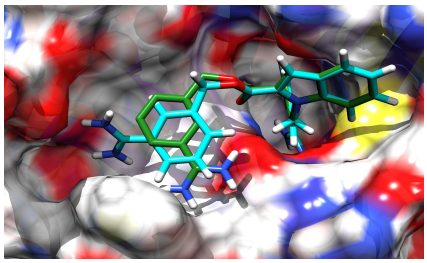
TOC graphics.